Analysis of a Scroll Machine for Micro ORC Applications by means of a RE/CFD Methodology

Mirko Morini

Dipartimento di Ingegneria Industriale, Università degli Studi di Parma

Parco Area delle Scienze, 181/A 43124 Parma, Italy

mirko.morini@unipr.it

Claudio Pavan

MechLav, Università degli Studi di Ferrara

via Saragat 1, 44122 Ferrara, Italy

claudio.pavan@unife.it

Michele Pinelli[1]

Dipartimento di Ingegneria, Università degli Studi di Ferrara

via Saragat 1, 44122 Ferrara, Italy

michele.pinelli@unife.it

Eva Romito

Dipartimento di Ingegneria, Università degli Studi di Ferrara

via Saragat 1, 44122 Ferrara, Italy

eva.romito@student.unife.it

Alessio Suman

Dipartimento di Ingegneria, Università degli Studi di Ferrara

via Saragat 1, 44122 Ferrara, Italy

alessio.suman@unife.it

ABSTRACT

In this paper an integrated Reverse Engineering - Computational Fluid Dynamics (RE/CFD) methodology is applied in order to study the adaptation of a commercial scroll compressor to be used as an expander in a micro ORC system. The analysis consists of the acquisition of a real scroll compressor geometry through an RE procedure, the

[1] corresponding author, phone +39 (0)532 974889

transient numerical simulation of the scroll in compression and expansion mode and the analysis of the performance in terms of pressure and mass flow rate profiles and volumetric efficiency. In order to set up the numerical strategy, a literature test case is used to perform a sensitivity analysis. The results obtained are: (i) the assessment of a numerical strategy with respect to the most critical parameters of a dynamic mesh-based simulation; (ii) the set up and validation of a Reverse Engineering-based numerical procedure; (iii) the evidence of the different fluid dynamic behavior of the scroll machine in compressor mode compared to the expander mode and (iv) the strong relationship between the volumetric efficiency of the scroll machine and the magnitude of the flank gap.

Keywords: ORC, Scroll, Reverse Engineering, CFD, Dynamic Mesh

INTRODUCTION

The scroll fluid machine has gained popularity since the 1970s as a compressor in air conditioning and refrigeration applications. Its main advantages are the small number of moving parts and its reduced noise and vibrations. Recently, this technology has gained renewed interest due to its potential adaptability to be used as an expander in micro ORC systems. In particular, the concept was reinvented to build scroll air motors (expanders), which are adopted to drive generators for electric power generation because of the scroll inherent advantages.

The ever-increasing request for higher efficiency in machine operation (e.g. eco-design) has led to the need for designers to thoroughly investigate the kinematic and thermodynamic behavior of these machines by means of geometric, thermodynamic and, very recently, CFD methods.

The relationship between the scroll spiral profiles and, therefore, scroll pockets evolution, and the machine overall performances both in terms of energy and mechanics is the first step towards understanding scroll machine working behavior. This preliminary analysis is not possible by using a classic approach (in which the mathematical definition of the scroll spiral profile allows the calculation of the pocket volume and its evolution with the orbit angle) in the case of a commercial machine, bought as it is on the market. In this case, a new methodology, called Reverse Engineering, represents a very useful method for generating a computational geometry of the real machine. As mentioned above, the ever-increasing demand for high energy efficiency standards and low production costs, determines the necessity to understand every aspect of the machine in terms of performance, materials and, no less important, noise and vibration. Domestic and micro-industrial applications represent the last challenge for energy recovery and micro power-plant design.

In this paper, a real scroll compressor geometry is studied by means of a Reverse Engineering (RE)-Computational Fluid Dynamic (CFD) procedure and analyzed in compression and expansion mode. The scroll geometry acquired is the

commercial SANDEN TRSA09-3658 scroll compressor. Preliminarily, a test geometry is obtained by means of a literature mathematical model and used in order to assess and set up a numerical strategy which makes use of a Dynamic Mesh (DM) approach to simulate the transient behavior of the machine. The numerical strategy is carried out through a sensitivity analysis performed on the numerical time step (angular increment) of the rotating machine which, in turn, is related and influences the topology and the quality of the mesh. Then, the real geometry is analyzed and the results presented in terms of pressure and mass flow rate fluctuations, overall volumetric efficiency both in compressor and expansion mode and influence of the flank gaps on the scroll performance.

In synthesis, the main contributions of this paper are:

- the application to a real world scroll machine of a *combined* Reverse Engineering/Computational Fluid Dynamic methodology which allowed the obtainment of information rarely available either in literature or from manufacturer data, such as flank gaps, actual geometric features of scroll profile nose. Moreover, the RE allowed the obtainment of the scroll profiles without relying on theoretical mathematical models, which could be significantly different from the manufactured ones;
- the implementation of a inventive Dynamic Mesh computational strategy which, making use of the actual flank gaps derived from the RE, allowed the resolution of the numerical model when very small (always lower than 100 μm with a minimum as equal to 20 μm) and variable-with-orbit flank gaps, while usually in literature the flank gaps are modelled as fixed and by using values greater than 100 μm. Moreover, in the paper, a method for the obtainment of the pressure-angle curve from the DM raw data is illustrated;
- the comparison between the compression and expansion operating mode of the same geometry, which can give information on the possibility of effective conversion from compressor to expander, and vice versa, of a real commercially available machine.

LITERATURE REVIEW

In literature, the study of positive displacement operating machines is mostly performed through experimental tests. Recently, CFD applications have been increasingly proposed, thanks to the evolution of dynamic mesh capability both in terms of algorithms and computational resources. Scroll machines are treated almost exclusively through experimental approaches, while there is still a lack of CFD analysis due to the particular complexity of the machine geometry and of its working mode. The application of RE approach is an ever increasing methodology in fluid machinery studies, but its application in conjunction with the CFD approach is the early stage when dealing with small size positive displacement machines. Recently, the authors have presented a RE/CFD analysis in which the CFD data are used for the setup of a lumped parameter model of a ORC cycle for domestic applications [1].

The earliest applications of experimental small size ORC systems considered the ORC as a system component dedicated to a specific mode of utilization. For example, in [2] the development of a demonstration package that supply residential cooling and electricity via a solar-heated Rankine cycle is reported. Then, in order to meet the increasing demands of efficiency and cost, the need for an experiment dedicated to each individual component of the energy system arose. In fact, in many cases, the individual components are derived from applications other than those for which they are originally used.

For these reasons, laboratory micro- and sub-systems have been developed in order to study and optimize the entire energy system starting from *ad hoc* designed prototypes. In particular, a number of applications concerns small- and micro- size systems (<10 kWe), for which the achievement of engineered solutions is particularly difficult.

The complete review proposed by Bao and Zhao [3] pointed out that for micro-system energy, the volumetric expander technology is the most preferable in terms of efficiency and cost. In particular, for applications in the range of (1—10) kWe, scroll, screw and rotary vane expanders are the most suitable for the ORC power-plants.

In the last five years, many ORC applications that involved the scroll expander have been presented. Categorizing the experimental rigs with respect to the scroll expander power, three ranges of power can be identified: (i) power range from 1.82 kW to 2.10 kW (in [4] an open-drive oil-free air scroll compressor with a 4.05 built-in volume ratio was used, in [5] an hermetic scroll compressor design for heat pump applications with a 3.00 built-in volume ratio was used and in [6] an air scroll compressor with a 3.95 built-in volume ratio was used), (ii) power range from 0.835 kW to 1.50 kW (in [7] a semi-custom, commercially derived scroll expander with a 2.5 expansion ratio was used, in [8] a in-house designed scroll compressor was used and in [9] a modified hermetic scroll compressor was used), and (iii)) power range from 98 W to 256 W (in [10] a commercially derived scroll with a 4.57 mechanical expansion ratio was used, while in [11] the ORC application refers to an pumpless cycle where the power generation is controlled by a smart valve system).

The performances of the volumetric expander are related, in particular, to the variation of the isolated volumes during rotation and the seals. The relationship between the scroll spiral profiles and, therefore, scroll pockets evolution and the machine overall performances both in terms of energy and mechanics is the first step towards understanding scroll machine working behavior. Examples of the spiral design can be found in literature. Different points of view are adopted by the authors in order to create the best compromise between efficiency and mechanical integrity of the scroll. In [12] a practical design on the 5,200 – 9,800 W capacity range of the scroll-type compressor family is proposed while in [13] a design procedure, combining the geometry of the scroll profiles constructed from an involute of circle with variable radii is proposed. In [14] the scroll profiles mathematical model is characterized by linear equations governed by linear coefficients that allows the obtainment of constant thickness profiles with respect to the spiral angle. In [15],

the Perfectly Meshing Profile (PMP) method for the design of the scroll nose profile is proposed and outlined. In cases where the mathematical model is not available, (e.g. in the case of commercial devices) the chance to know the actual spiral profile is related to the re-construction capability of the user.

The RE method has recently gained importance in product development, maintenance/recovery and re-manufacturing fields. Some examples can be found in [16], where the RE method was used for different objects for which the CAD-3D support did not exist. The RE procedure and instruments have improved their accuracy in recent years and, at the same time, the progress in software development allows three-dimensional representation of the real object to be obtained in a very short time.

A very recently interesting review is presented in Song *et al.* [17]. In their work, the Authors states that CFD simulation for the scroll machine is still in early stage because of the complex geometry and unique motion of orbiting scroll wrap, which is also one of the main issues (in particular, the second key issue of CFD applications stressed in [17]) faced in the present paper.

The use of 2D CFD analysis by using a Dynamic Mesh for studying the turbulence in the suction chamber and the cavitation phenomena of a gear pump can be found in literature. In particular, in [18] the attention was given to the turbulence structure in the suction chamber, while in [19] the analysis referred to the pressure variation and cavitation phenomena. In these cases, the 2D strategy allows the comprehension of the major fluid dynamic phenomena involved in volumetric devices. A three dimensional application with Dynamic Mesh strategy can be found in [20], where the transient simulation is adopted in order to point out the power losses generated by the lubricant in a gear box. Regarding the scroll machine, the use of CFD methods for the evaluation of scroll machine performance is not widespread in literature. For example, Cui [21] has performed an analysis oriented to the evaluation of the pressure distribution in the pockets and in the leakages through the flank gap.

In this context, the validity of 2D versus 3D simulation is still an open question. In fact, in [17], the authors claim that 2D numerical models cannot reflect the accurate spatial distribution and variation of the flow field. At the same time, in [22], the authors demonstrated that the pressure variation on the expansion process by 2D geometry is slightly higher than that of 3D model, but the overall tendency is similar and the deviation is acceptable. In the opinion of the authors of the present paper, 2D simulation can help in a first design phase when thermodynamic cycle parameters and pressure and mass flow rates fluctuation at the inlet and outlet port have to be analyzed, while 3D approach is essential when detailed fluid dynamic features (regarding in particular the axial clearance gaps, if present) and machine performance parameters (such as volumetric efficiency) have to analyzed for the subsequent machine optimization.

LITERATURE CASE STUDY

In order to set up the numerical strategy and to choose the most appropriate time-step (or angular step) amplitude for the subsequent analysis on the real scroll machine, a preliminary analysis has been carried out on a case study geometry. The geometry has been generated by means of a mathematical model derived from literature. This approach has been chosen since a mathematically-generated geometry is more suitable for numerical sensitivity analysis. In fact, a geometry reconstructed by means of a measuring device is affected by measuring errors and real world effects (such as irregularities, local deformations, manufacturing tolerances, etc.) which can hide the sensitivity to the numerical solution. The authors have performed this CFD analysis by using the same strategy (Dynamic Mesh) adopted for the real scroll, while numerical domain and mesh were generated for the two geometries individually. The case study scroll machine has been performed in compression mode only.

Profile design method. The method, proposed in [14], is characterized by linear equations governed by linear coefficients. This particularity allows the obtainment of constant thickness profiles with respect to the spiral angle. This method is the evolutions of the Involuted Circle Method, in which the spiral curve radius is assumed to vary with a linear law starting from a base circumference centered in the origin of the reference system. To connect the inner and outer profile of the spiral, the Perfectly Meshing Profile (PMP) method was used [15]. The PMP allows the nose of the scroll profile to be shaped in a continuous and regular way.

Table 1 summarizes (i) the values of all the coefficients used for the generation of the geometries, (ii) the resulting dimensions of the scroll obtained according to the adopted method and (iii) the parameter used in the PMP method. The PMP method allowed the thickening of the blade in order to have greater structural strength and to reduce leakage flows. All the geometric features reported in Tab. 1 influence the overall performance of the scroll device. The volume ratio of the case study scroll geometry is equal to 2.53.

Numerical strategy. The CFD simulations were carried out as a 2D transient numerical model by using a Dynamic Mesh (DM) strategy. This transient analysis is able to reproduce the real operation of the machine through a sequence of relative positions between the fixed and moving profile by imposing an angular increment $\Delta\theta$. With the DM strategy, the mesh inside the fixed and moving (orbiting) profiles is regenerated at each time step to accommodate the shape and size change of the gas pockets.

The mesh was composed of about 302,000 triangular elements. The maximum element skewness of the initial mesh is smaller than 0.47 (0.60 before smoothing) and a minimum orthogonal quality at least equal to 0.68 was achieved. To increase the resolution of the mesh close to the walls, a local mesh refining approach was adopted. The local refining around the walls is shown in Fig. 1. In the flank gap there are at least two triangular mesh elements. This value is in line with those reported in literature [18, 19] for volumetric displacements.

The software used for this analysis is Ansys Fluent 13.0. To perform the bi-dimensional CFD simulations, the outlet (compressor mode) boundary condition has been imposed in correspondence to the central volume of the machine by means of an opening section. In Fig. 1, the detail of the central volume of the scroll in which the outlet section has been placed is presented.

The simulations were conducted by imposing a pressure ratio of 3.5. The reference pressure is 101,325 Pa. The rotational velocity was imposed equal to 2,000 rpm. The turbulence model chosen, in accordance with [23], is the k-ε model combined with standard wall functions.

A sensitivity analysis on the value of $\Delta\theta$ was performed by imposing four different values, i.e. $\Delta\theta = 0.2500°$, $0.1250°$, $0.0625°$ and $0.0417°$. The mesh deformation is closely related to the amplitude of the displacement that is imposed on the moving scroll. In Fig. 2, it can be seen that an increase of the angular increment results in higher deformations of the mesh and, then, of different maximum skewness values S during the orbit. Also, in Fig. 2 the average skewness values S^* are reported. As can be seen in Fig. 2, each CFD simulation considers three complete orbits of the scroll, which allows the achievement of a periodic working condition. The results are related to the second and third orbit of the transient simulation.

Results and discussion. In Fig. 3, the results referring to the mass flow rate and pressure at the suction, as a function of the orbit angle, are presented. At the suction, the simulation for $\Delta\theta = 0.1250°$ presents greater fluctuations compared to other $\Delta\theta$, but the trend is comparable with that obtained from the other simulations. This phenomenon, however, does not occur at the discharge where the four trends of the mass flow rate are superimposed (not shown in the Figures). In Fig. 3, values of the pressure at the compressor suction referring to a monitoring point (shown as a star symbol in the figure) are presented. The same behavior already noticed for the mass flow rate at $\Delta\theta = 0.1250°$ is highlighted.

In addition, a significantly higher pressure for the simulation at $\Delta\theta = 0.0625°$ can be noticed. This phenomenon can be due to the fact that wide recirculation zones with reversed flow are always present at the machine suction and, thus, the pressure values at the monitoring point can be affected by the local solution. The recirculation phenomena and reversed flow are reported in Fig. 4.

The analysis showed that overall performances are not influenced by the angular increment $\Delta\theta$, but local mesh deformation can lead to different local fields of pressure and velocity. After this sensitivity analysis, the chosen angular increment was $\Delta\theta = 0.0625°$. The equivalent time step is then $\Delta t = 5.21\ 10^{-6}$ s adopted for all the following simulations on the real scroll device. This time step permits a good compromise between computational effort and a reliable solution.

REAL SCROLL DEVICE

The CFD analyses for the Sanden scroll compressor are carried out with the same strategy presented above. Then all the following analyses are conducted with a transient simulation with a DM approach. The computational domain is based on the real geometry obtained by a reverse engineering procedure. The computational strategy is similar to the previous CFD analysis and the results are referred to the scroll device that works in compressor and expander mode.

Real geometry design. The real geometry of the Sanden TRSA09-3658 scroll was obtained through an RE procedure. The RE of the real component has been performed by means of a Romer laser scanner and the subsequent parametric CAD representations. At first, a 3D polygonal geometry is obtained by interpolating the point cloud derived from the laser scanner by means of the Polyworks V12 software.

In Tab. 2 the scroll compressor geometrical characteristics are reported while in Fig. 5, a real scroll device is shown. As can be seen from Tab. 2, the scroll flank gaps are non-uniform flank gaps during the orbit. Some considerations can be drawn after the RE procedure:

- before RE, no evidence of variable-with-orbit flank gap was expected. Usually, at the design stage, the flank gaps are considered constant. Their variability observed on the actual machine, after RE, can be due to: (i) the physiological discrepancy between ideal CAD geometry and actual geometry after manufacturing; (ii) the actual geometry of the stator and rotor assembly during standard working operation; (iii) the error inherent to the laser scanner device and to the subsequent interpolating process of the cloud points. Nevertheless, the RE procedure was considered reliable and the values of the flank gaps, even affected by experimental uncertainty, were considered consistent;
- the maximum inlet volume of the Sanden scroll compressor delivered by the manufacturer is different from the measured one. In particular, the manufacturer value is equal to 85,700 mm^3. The discrepancy between the two values is equal to 200 mm^3. After an order of magnitude calculation, this value was estimated to be equivalent to an uncertainty on the mass flow rate of about 1.5 %, which is acceptable if compared to typical experimental uncertainty on mass flow rate [23].

The computational domain consists of a bi-dimensional representation of the scroll machine. In fact, a 2D section has been obtained by intersecting the 3D polygonal model with a plane perpendicular to the rotation axis. The 2D section is then exported into the CAD software SolidWorks 2012 through an interchange file format, e.g .stp or .iges format. The scroll profile is then made regular and continuous by means of Spline curves.

The reproduction of the scroll as obtained by RE is shown in Fig. 6. In Fig. 6a the fixed profile and the moving profile are shown. In Fig. 6b, the 2D surface used for CFD simulation is outlined.

The spiral of the scroll in question was compared with a spiral obtained from the general equations found in [13], providing a good agreement between the two spirals up to an angular position of about $\theta = 270°$. As mentioned above, the scroll device is bought as it is on the market without knowing the real mathematical formulation of the spirals.

Mesh. The mesh was composed of about 900,000 triangular elements. The maximum element skewness of the initial mesh is smaller than 0.33 (0.60 before smoothing) and a minimum orthogonal quality at least equal to 0.655 was achieved. To increase the resolution of the mesh close to the walls, a local mesh refining approach was adopted. The local refining around the walls is shown in Fig. 7. In the flank gap there are two triangular mesh elements at least in agreement with the previous analysis. The geometry of the real scroll is similar to that of the literature case study and in addition, the numerical domain of the real scroll is discretized through the use of a triangular mesh topologically similar to that used for the test case numerical domain, in terms of element distribution and growth ratio. In this manner, the results related to the time step sensitivity analysis are suitable for the real scroll simulation.

Boundary conditions and turbulence model. The software used for this analysis is Ansys Fluent 13.0. To perform the bi-dimensional CFD simulations, the inlet (in the case of expansion operation) or outlet (in the case of compression operation) boundary condition has been imposed in correspondence to the central volume of the machine by means of an opening on the fixed profile. In Fig. 6c, the detail of the central volume of the scroll in which the outlet/inlet section has been placed is presented.

Both simulations (scroll as a compressor and scroll as an expander) were conducted by imposing a pressure ratio of 3.5. The reference pressure is 101,325 Pa. In Figs 8a and 8b pressure boundary conditions are summarized for scroll compressor and scroll expander. The rotational velocity was imposed equal to 2,000 rpm. The turbulence model chosen, in accordance with [21], is the k-ε model combined with standard wall functions. The fluid considered for the comparisons between the scroll compressor and the scroll expander analysis is air at standard conditions.

Simulation of scroll machines by using real gas equations is numerically very challenging and could drain most of the computational resources during the simulation. Moreover, the specific geometry under consideration is characterized by time-varying sliding narrow gaps which result in tough convergence issues when using air as the working fluid. These issues are even more relevant when refrigerant is used. For these reasons, for the purposes of this paper (i.e. sensitivity analyses and the setting up of an RE-CFD methodology) only air is considered as the working fluid. This methodology can also be found in literature for the experimental test. For example, in [9], the preliminary analyses for ORC devices were conducted by using air as the working fluid.

REAL SCROLL ANALYSIS

The results on the real machine are presented both in compressor and expander mode. The two working conditions are then compared to each other in order to detect the similarities and differences between the operating modes.

Pressure. In Fig. 9, the delivery pressure of the scroll compressor and the discharge pressure of the scroll expander are presented as a function of the normalized angular position of the orbit covered by the moving spiral profile. The scroll compressor shows a smooth trend in discharge pressure. Irregularities due to the interaction of the leakages with the delivery section obtained on the fixed profile can be appreciated at 75 % of the orbit, as can be seen in the pressure contour plot at the same orbit percentage. In any case, pressure value fluctuations are contained in few Pa.

On the contrary, the scroll expander shows a more irregular trend, with greater fluctuations of the pressure value at the exhaust. Also, in expansion operating mode, the asymmetry of the fluid pressure in the isolated pocket is more visible. In particular, in Fig. 9, the contour plots referring to the latter expander orbit angles (75 % and 100 %) show a different pressure for the twin discharge pockets. This phenomenon is related to the asymmetric position of the inlet and outlet ports and strongly linked to the design of the scroll machine.

Thanks to a particular procedure the entire fluid pressure variation inside the scroll machine can be reconstructed. By using twelve pressure control points it is possible to generate the overall trend of the pressure variation. Figure 10 shows the adopted procedure that can be summarized as follows: (i) definition of the pressure control points position, (ii) collection of the pressure data during the transient solution in each control point, (iii) representation of all pressure data and definition of the couple control point-orbit angle in order to generate an artificial continuous pressure data flow with respect to the orbit angle and (iv) representation of the pressure data flow as a function of the orbit angle. This procedure and therefore this data representation allow the definition of which pressure fluctuations affect the machine during standard operation. These results are very important to understand the vibration and noise generated by the machine.

Flow rate and velocity field. In Fig. 11, the mass flow of the scroll compressor and scroll expander are reported. The mass flow rate operated by the scroll expander is higher than the mass flow rate operated by the scroll compressor. This difference is due to the flank gaps that allow the fluid in the scroll expander to by-pass the moving scroll towards the discharge outlet. In Fig. 11, the evolution of the velocity fields inside the compressor/expander scroll are presented. From these plots, the back flow at the inlet port during compression mode can be clearly observed. This aspect seems to be due to the dimension of the external case of the scroll machine. This result may not be very representative of the actual scroll machine. In fact, in these bi-dimensional simulations the operation fluid does not have the possibility to move along the rotating axis of the machine, and thus, possible three dimensional flows are neglected from the results reported in this paper.

Volumetric efficiency. The volumetric efficiency of the scroll machine was also estimated by means of CFD results for both of the operation modes (compression and expansion).

The volumetric efficiency of the scroll compressor, η_{v_C}, was obtained as the ratio of the calculated volume flow rate operated by the scroll and the ideal volume flow rate obtained through the theoretical volumes isolated by the scroll compressor. This value resulted equal to 0.29, as a consequence of the imposed flank gap between the fixed and the moving profiles. This value is comparable to similar results found in literature [24].

The volumetric efficiency of the scroll expander, VFM (Volumetric Flow Matching ratio), was obtained as the ratio of the ideal volume flow rate determined through the theoretical volume isolated by the scroll and the CFD calculated volume flow operated by the scroll. The VFM value should be as close as possible to one for optimal performance. Greater values indicate higher volumetric losses. The VFM resulted equal to 3.06. This high value, consistent with the data presented in [24], is closely related to the value of the flank gap imposed between the fixed scroll and the moving scroll.

As previously mentioned, the magnitude of the flank gap influences the performance of the scroll machine (in particular the volumetric efficiency). By using the CFD simulations, leakage flows in the flank gap, that affect the operation of both machines, can be clearly observed. In Fig. 12 there are two representations of the flank leakage that affect the scroll expander. In this operation mode, the fluid overpasses the spiral through the flank gaps without energy exchanges (and thus work) with the mobile spiral. Figure 12 shows the flank leakages (i) from the discharge chamber to the outlet volume (casing), (ii) from the expansion chamber to the discharge chamber and finally (iii) from the suction chamber to the expansion chamber.

The flank leakages are, in general, driven by (i) the magnitude of the flank gaps, (ii) the density of the operating fluid, (iii) the presence of the lubricating oil and (iv) the pressure difference between two consecutive isolated pockets. In general long spirals allow the reduction of the pressure difference between two consecutive isolated pockets (and thus there is less flank leakage) but the scroll machine becomes bigger and more expensive. In the same way, the use of lubricating oil allows the reduction of leakages thanks to its phase (liquid) and viscosity but the scroll machine and, in this case, the entire circuit become more complicated and expensive. For this solution, in fact, it is necessary to design special components for the circuit (such as an oil separator) or modify the preliminary design of the standard ones (such as the heat exchanger).

CONCLUSIONS

In this paper a comprehensive performance and fluid dynamic assessment of a real scroll machine was presented by means of CFD analyses. The study was related to two operating modes of the scroll machine: compression and expansion modes.

Thanks to the use of a reverse engineering procedure, an unknown scroll compressor geometry was reconstructed and digitalized. The use of CFD simulation allows the study of the detailed working features of the machine that are not completely visible with other types of analyses (such as thermodynamic or lumped approach).

A CFD method was developed by means of a transient dynamic mesh strategy. The CFD transient simulations allowed the evaluation of time profile of the mass flow rate and pressure fluctuations at the inlet and outlet sections of the machine.

A sensitivity analysis on the simulation parameters has been carried out in order to optimize the CFD strategy for the simulation of scroll machines. For this analysis, a scroll machine reported in literature has been adopted. The analysis showed that overall performances are not influenced by the angular increment $\Delta\theta$, but local mesh deformation can lead to different local fields of pressure and velocity.

The analyses on the real scroll machine have shown (i) asymmetric distributions of the pressure inside the scroll pocket, (ii) backflow at the inlet port during the compression mode and (iii) velocity magnitude of the flank leakages due to the flank gaps. All of these phenomena impact on the scroll performance, and only through their comprehension it is possible to optimize the scroll design by the modification of the spiral profile or the position and dimension of the inlet and outlet port. An important aspect is linked to the pressure fluctuations that are closely related to vibrations and noise generated by the machine in operation. These aspects play an important role in the case of household appliances, where the vibration and noise are as critical parameters as energy efficiency.

Further developments are related to the full three-dimensional CFD simulations of the real scroll machine and the comparison of its simulated performance with those obtained from other volumetric machines, such as screw or gear pumps.

ACKNOWLEDEGMENT

The research was partially supported by the Italian Ministry of Economic Development within the framework of the Program Agreement MSE-CNR “Ricerca del Sistema elettrico nazionale (RdS)”.

NOMENCLATURE

m	mass flow rate
P	control point

p pressure

S skewness

t time

v velocity

Greek letters

θ orbit angle

Δ step

η efficiency

Superscript and Subscript

C compressor

E expander

v volumetric

* average

Acronyms

DM Dynamic Mesh

PMP Perfect Meshing Profile

RE Reverse Engineering

VFM Volumetric Flow Matching ratio

REFERENCES

[1] Ziviani, D., Suman, A., Lecompt, S., De Paepe, M., van den Broek, M., Spina, P. R., Pinelli, M., Venturini, M., Beyene, A., 2014, "Comparison of a Single-Screw and a Scroll Expander under Part-Load Conditions for Low-Grade Heat Recovery ORC Systems", Proc. of 6th International Conference on Applied Energy (ICAE2014), Taipei, 30 May - 2 June, 2014, Paper n. 78, pp. 1-4.

[2] Prigmore, D., Barber, R., 1975, "Cooling with the sun's heat", *Solar Energy*, **17**, pp. 185-192

[3] Bao, J., Zhao, L., 2013, "A review of working fluid and expander selections for organic Rankine cycle", *Renewable and Sustainable Energy Reviews*, **24**, pp. 325-342

[4] Lemort, V., Quoilin, S., Cuevas, C., Lebrun, J., 2009, "Testing and modeling a scroll expander integrated into an Organic Rankine Cycle", *Applied Thermal Engineering*, **29**, pp. 3094-3102

[5] Lemort, V., Declaye, S., Quoilin, S., 2012 “Experimental characterization of a hermetic scroll expander for use in a micro-scale Rankine cycle”, *Proceedings of the Institution of Mechanical Engineers, Part A: Journal of Power and Energy*, **226**, pp. 126-136

[6] Declaye, S., Quoilin, S., Guillaume, L., Lemort, V., 2013, “Experimental study on an open-drive scroll expander integrated into an ORC (Organic Rankine Cycle) system with R245fa as working fluid”, *Energy*, **55**, pp. 173-183

[7] Wang, H., Peterson, R. B., Herron, T., 2009, “Experimental performance of a compliant scroll expander for an organic Rankine cycle”, *Journal Power and Energy*, **223**, pp. 863-872

[8] Harada, K. J., 2010, “Development of a Small Scale Scroll Expander”, Master of Science Thesis in Mechanical Engineering, Oregon State University, Oregon, US,. http://hdl.handle.net/1957/18837.

[9] Bracco, R., Clemente, S., Micheli, D., Reini, M., 2013, “Experimental tests and modelization of a domestic-scale ORC (Organic Rankine Cycle)”, *Energy*, **58**, pp. 107-116

[10] Peterson, R.B., Wang, H., Herron, T., 2008, “Performance of a small-scale regenerative Rankine power cycle employing a scroll expander”, *Journal of Power and Energy*, **222**, pp. 271-282

[11] Yamada, N., Watanabe, M., Hoshi, A., 2013, “Experiment on pumpless Rankine-type cycle with scroll expander”, *Energy*, **49**, pp. 137-145

[12] Tseng, C. H., Chang, Y. C., 2006, “Family design of scroll compressors with optimization”, *Applied Thermal Engineering*, **26**, pp. 1074-1086

[13] Liu, Y. et al., 2012, “Optimum design of scroll profiles created from involute of circle with variable radii by using finite element analysis”, *Mechanism and Machine Theory*, **55**, pp. 1-17

[14] Blunier, B. et al., 2006, “Novel Geometrical Model of Scroll Compressors for the Analytical Description of the Chamber Volumes”, Proc.of 18th International Compressor Engineering Conference; Purdue, USA, Jul 15-20, 2006, Paper 1745, http://docs.lib.purdue.edu/icec/1745

[15] Liu, Y. et al., 2010, “Study on involute of circle with variable radii in a scroll compressor”, *Mechanism and Machine Theory*, **45**, pp. 1520-36

[16] Bagci, E., 2009, "Reverse engineering applications for recovery of broken or worn parts and re-manufacturing: Three case studies", *Advances in Engineering Software*, **40**, pp. 407-418

[17] Song, P., Wei, M., Shi, L., Danish, S. N., Ma, C., 2015, “A review of scroll expanders for organic Rankine cycle systems”, *Applied Thermal Engineering*, **75**, pp. 54-64

[18] Castilla, R., Gamez-Montero, P. J., Ertürk, N., Vernet, A., Coussirat, M., Codina, E., 2010, “Numerical simulation of turbulent flow in the suction chamber of a gearpump using deforming mesh and mesh replacement”, *International Journal of Mechanical Sciences*, **52**, pp. 1334-1342

[19] Del Campo, D., Castilla, R., Raush, G. A., Gamez-Montero, P. J., Codina, E., 2012, "Numerical Analysis of External Gear Pumps Including Cavitation", *Journal of Fluids Engineering*, **134**, p. 081105

[20] Gorla, G., Concli, F., Stahl, C., Höhn, B. R., Michaelis, K., Schultheiß, H., Stemplinger, J. P., 2013, "Hydraulic losses of a gearbox: CFD analysis and experiments", *Tribology International*, **66**, pp. 337-344

[21] Cui, M. M., 2006, "Numerical Study of Unsteady Flows in a Scroll Compressor", *Journal of Fluids Engineering*, **128**, pp. 947-55

[22] Chang, J. C., Chang, C. W., Hung, T. C:, Lin, J. R., Huang, K. C., 2014, " Experimental study and CFD approach for scroll type expander used in low-temperature organic Rankine cycle", *Applied Thermal Engineering*, **73**, pp. 1444-1452

[23] Matos, M. A., Rodrigues, N., 2013, "Gas mass-flow meters: Measurement and uncertainties", *Flow Measurement and Instrumentation*, **33**, pp. 45-54

[24] Mathias, J. A., Johnston, J. R. J., Cao, J., Priedeman, D. K., Christensen, R. N., 2009, "Experimental Testing of Gerotor and Scroll Expanders Used in, and Energetic and Exergetic Modeling of, an Organic Rankine Cycle", *Journal of Energy Resources Technology*, **131**, p. 012201

TABLE CAPTIONS

Table 1. Coefficients, dimensions and PMP parameters used for the generation of the scroll

Table 2. Scroll compressor characteristics

FIGURE CAPTIONS

Figure 1. Computational domain of the sensitivity analysis and the mesh close to the outlet section

Figure 2. Maximum skewness values and the average skewness S* during the scroll orbit

Figure 3. Mass flow rate and pressure at the suction section of the literature compressor scroll

Figure 4. Recirculation zone at the suction side of the literature scroll compressor

Figure 5. Scroll SANDEN TRSA09-3658

Figure 6. Scroll geometry reconstruction: a) fixed (red) and moving (blue) profile, b) 2D surface and c) particular of the inlet/outlet port

Figure 7. Local mesh refinement around the scroll edge

Figure 8. The scroll boundary conditions. a) scroll compressor and b) scroll expander

Figure 9. Outlet pressure and pressure fields during the orbits

Figure 10. Pressure reconstruction for the scroll compressor

Figure 11. Mass flow rate and velocity fields

Figure 12. Flank leakages in the scroll expander

Table 1. *Coefficients, dimensions and PMP parameters used for the generation of the scroll*

Coefficient	Value	Geometric		Value
Radius of based circle [mm]	4.428	Orbiting radius [mm]		10.430
Corrected increment [mm]	-	Orbiting scroll min endplate diameter [mm]		178
Scroll pair wrap height [mm]	56.0	Orbiting scroll endplate diameter [mm]		185
Ended involute angle [rad]	16.93	Thickness [mm]		3.480
Inner curve initial angle [rad]	0.785	PMP	Inner curve starting involute angle [rad]	3.770
Inner curve initial angle [rad]	0.000	PMP	Outer curve starting involute angle [rad]	0.350

Table 2. Scroll compressor characteristics

Volume ratio	3.1055	
Maximum inlet volume [mm^3]	85,900	
Spiral height [mm]	33.5	
End-plate diameter [mm]	120.0	
Axial duct diameter [mm]	12.0	
Radial duct diameter [mm]	12.5	
Flank gap [μm]	**0° (inlet chambers close)**	20
	90°	36
	180°	94
	270°	36

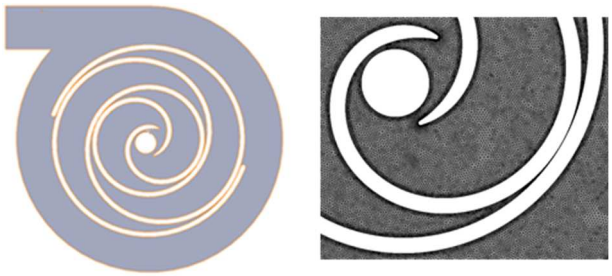

Figure 1. Computational domain of the sensitivity analysis and the mesh close to the outlet section

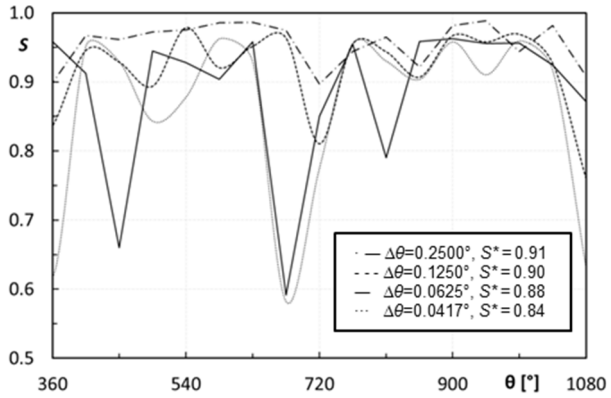

Figure 2. Maximum skewness values and the average skewness *S** during the scroll orbit

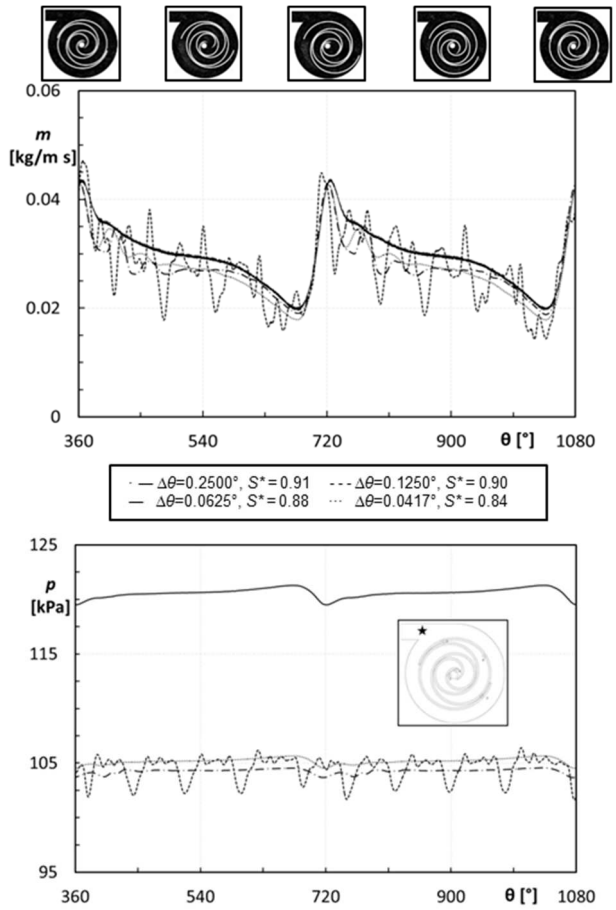

Figure 3. Mass flow rate and pressure at the suction section of the literature compressor scroll

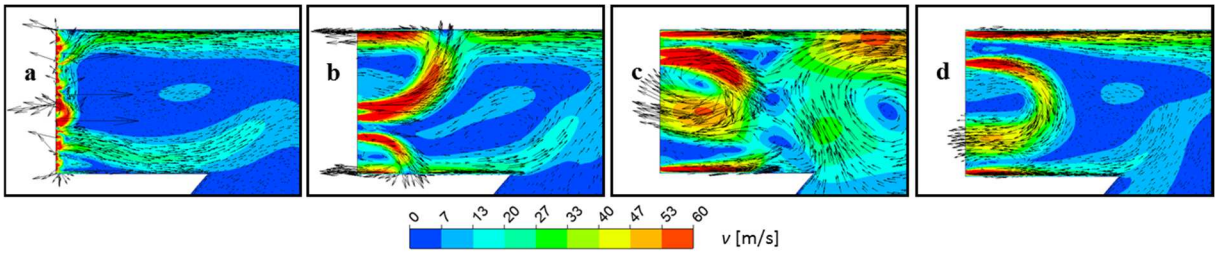

Figure 4. Recirculation zone at the suction side of the literature scroll compressor

Figure 5. Scroll SANDEN TRSA09-3658

Figure 6. Scroll geometry reconstruction: a) fixed (red) and moving (blue) profile, b) 2D surface and c) particular of the inlet/outlet port

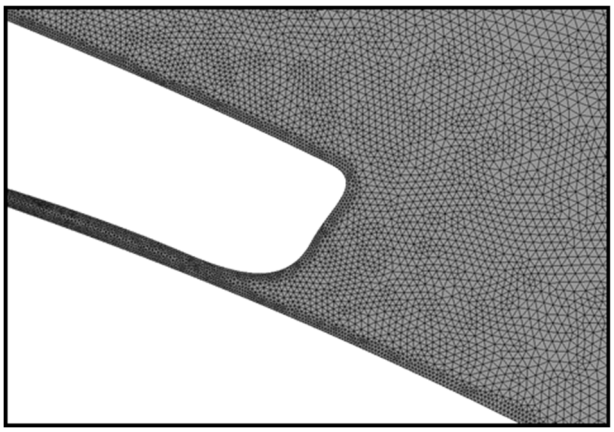

Figure 7. Local mesh refinement around the scroll edge

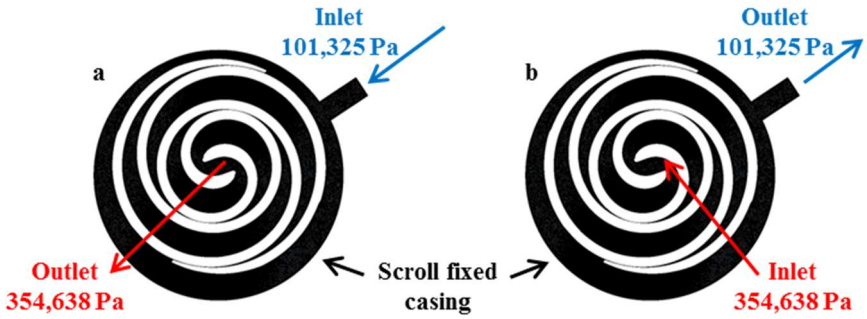

Figure 8. The scroll boundary conditions. a) scroll compressor and b) scroll expander

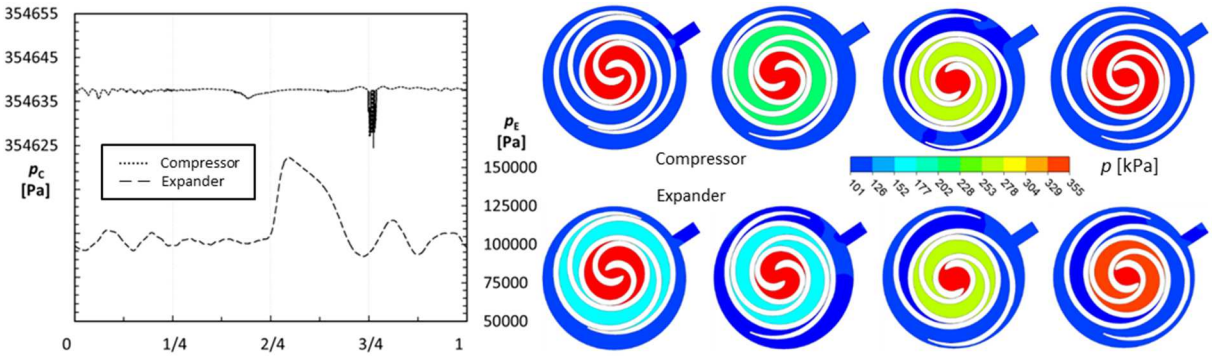

Figure 9. Outlet pressure and pressure fields during the orbits

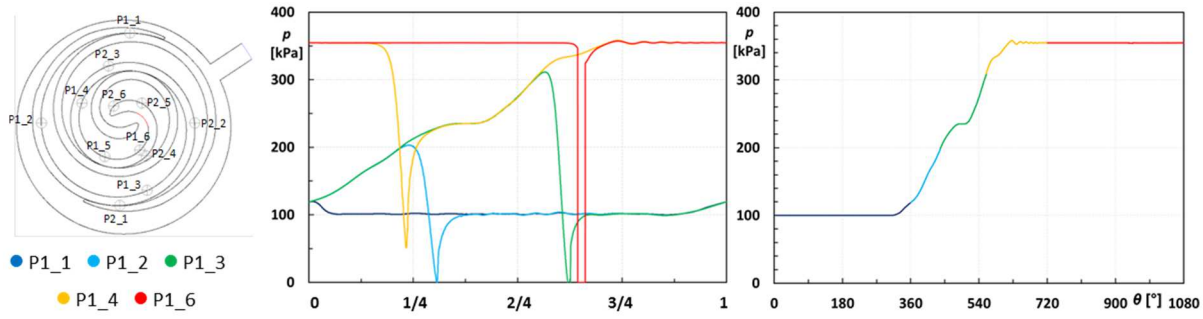

Figure 10. Pressure reconstruction for the scroll compressor

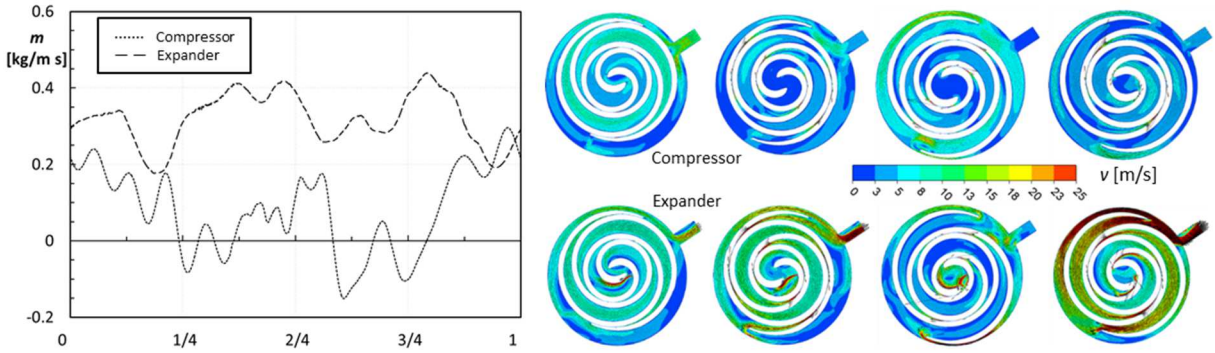

Figure 11. Mass flow rate and velocity fields

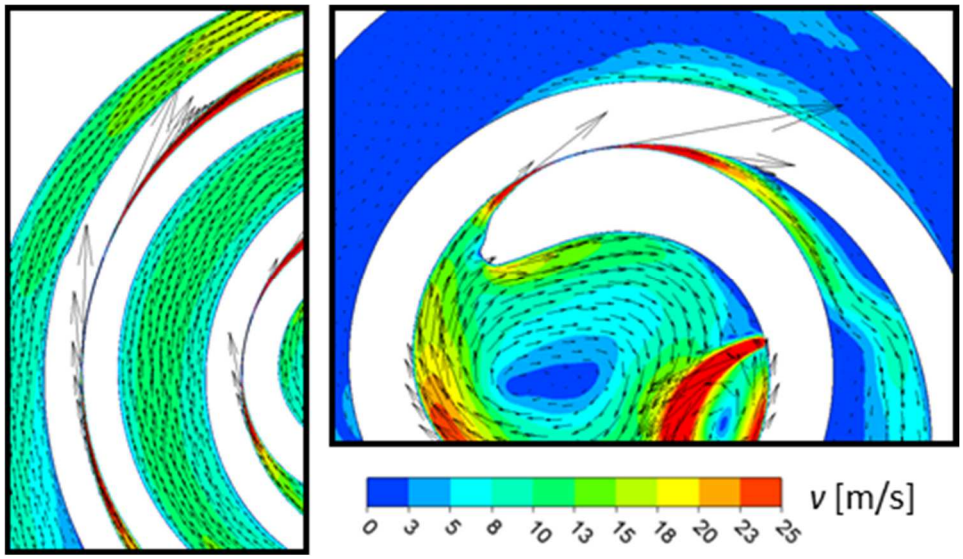

Figure 12. Flank leakages in the scroll expander